

# SiamSNN: Spike-based Siamese Network for Energy-Efficient and Real-time Object Tracking

Yihao Luo, Min Xu, Caihong Yuan, Xiang Cao, Liangqi Zhang, Yan Xu, Tianjiang Wang and Qi Feng

**Abstract**—Recently spiking neural networks (SNNs), the third-generation of neural networks has shown remarkable capabilities of energy-efficient computing, which is a promising alternative for deep neural networks (DNNs) with high energy consumption. SNNs have reached competitive results compared to DNNs in relatively simple tasks and small datasets such as image classification and MNIST/CIFAR, but there are few studies on more challenging vision tasks on complex datasets. In this paper, we focus on object tracking, which is widely applied in various scenarios and has energy-saving and real-time requirements. In SNNs, it is a more challenging similarity estimation problem. Specifically, we present a spike-based Siamese network for energy-efficient and real-time tracking, called SiamSNN, where we propose an optimized hybrid similarity estimation method in the SNNs, and introduce a novel two-status coding scheme to optimize the temporal distribution of output spike trains for further improvement in performance. Our experiments show that SiamSNN achieves short latency and low precision loss of the original SiamFC on the tracking datasets OTB-2013, OTB-2015, and VOT2016. Moreover, SiamSNN achieves real-time (50 FPS) and extremely low energy consumption on TrueNorth.

**Index Terms**—Spiking neural networks, object tracking, temporal information, real-time.

## I. INTRODUCTION

NOWADAYS Deep Neural Networks (DNNs) have shown remarkable performance in various scenarios [1], [2], [3]. However, it is difficult to employ DNNs on embedded systems such as mobile devices due to the high computation cost and heavy energy consumption. To this end, many tiny but efficient networks [4], [5] are proposed and achieve promising performance. However, the problem of insufficient computing power still exists in resource-constrained systems.

As an alternative, spiking neural networks (SNNs) have realized ultra-low power consumption on neuromorphic hardware (such as TrueNorth [6] and Loihi [7]) by transmitting information in the form of an event-driven binary spike train rather than continuous values like DNNs [8]. Furthermore, spiking neurons in SNNs only fire an output spike when their membrane potentials exceed a certain threshold [9], which sparsely activates neurons in networks to save energy. SNNs are regarded as the third generation artificial neural networks

[10] because they are bio-inspired and more like a real human brain than the common DNNs.

SNNs have shown effectiveness in some scenarios, but there is still a gap to DNNs owing to the hardness of training [11]. One major reason is that the training algorithms, such as STDP [12] and backpropagation [13], can only train shallow SNNs with two or three layers. To avoid this issue, an alternative way is converting trained DNNs to SNNs [14], [15], [16]. This aims to convert DNNs to SNNs by transferring the well-trained models with weight rescaling and normalization methods, and there would only be a small loss of accuracy compared to original DNNs. Recently [17] achieves near-lossless conversion in image classification. Although SNNs have shown excellent potential, they have been limited to relatively simple tasks and small datasets (e.g., image classification on MNIST and CIFAR) [18], [19].

SNNs approaches that provide competitive results mostly in classification but few studies focus on other vision tasks, natural language processing, and reinforcement learning [20]. Most critically, the insufficiency of spike-based modules for various functions outside classification limits their applications, it is necessary to enrich them for greater prevalence. For instance, by converting leaky-ReLU to a spiked fashion and proposing a normalization method for regression problems, Spiking-YOLO [18] first performs object detection successfully on deep SNNs. In addition, SNNs of remarkable performance through conversion usually requires long latency [16], [21], which causes the inability to reach real-time requirements. Exploiting the sparse and temporal dynamics of spike-based information is significant to achieve real-time algorithms [20].

In this paper, we focus on object tracking in deep SNNs with the method of DNN-to-SNN conversion. Object tracking is valuable in various applications like traffic control [22], automatic driving [23], and video surveillance [24], which aims to estimate the target position in a sequence of frames with an object bounding box for the first frame. It is regarded as more challenging due to occlusions, deformation, background cluttering, and other distractors [25]. The state-of-the-art tracking models [26], [27] require high-performance GPUs, which involve a drastic increase in computation and power requirements that tends to be intractable for embedded platforms [28]. By the aid of energy-efficient computing in SNNs, implementing a spike-based tracker is significant to realize energy-efficient tracking algorithms on embedded systems, which also extends the limitations of current applications of SNNs. To realize it, two issues arise: (1) lack of the efficient similarity estimation function in SNN fashion; (2) hard to achieve comparable performance with common DNN-to-SNN

This work was supported in part by the National Nature Science Foundation of China under Grant 61572214. (Corresponding author: Qi Feng.)

Y. Luo, M. Xu, X. Cao, Y. Xu, T. Wang and Q. Feng are with School of Computer Science and Technology, Huazhong University of Science and Technology, Wuhan, Hubei, 430074, China (email: luoyihao@hust.edu.cn; simyhsu@hust.edu.cn; caoxiang112@hust.edu.cn; zhliangqi@hust.edu.cn; yanxu@hust.edu.cn; tjwang@hust.edu.cn; fengqi@hust.edu.cn).

C. Yuan is with School of Computer and Information Engineering, Henan University, Kaifeng 475004, China (email: yuanch@henu.edu.cn).

conversion methods.

To the first issue, we introduce an optimized hybrid similarity estimation method in the SNN fashion. The proposed method evaluates the similarity between feature maps of the exemplar image and candidate images in the form of spike. To the second problem, inspired by the neural phenomenon of long-term depression (LTD) [29], we design a two-status coding scheme to optimize the temporal distribution of output spike trains, which utilizes temporal information for shortening the latency to reach real-time and mitigating the accuracy degradation. Eventually, we present a spike-based Siamese network for object tracking called SiamSNN based on SiamFC [3]. To the best of our knowledge, SiamSNN is the first deep SNN for object tracking that achieves short latency and low precision loss of the original SiamFC on the tracking datasets OTB-2013 [30], OTB-2015 [31], and VOT2016 [32]. The contributions of this paper can be summarized as follows:

- We design SiamSNN for object tracking in deep SNN with short latency and low precision loss. This is the first successful attempt to apply deep SNN to object tracking on the datasets with complex scenes.
- We exploit temporal information of spike trains and propose an optimized hybrid similarity estimation method to construct a spike-based correlation layer, which efficiently evaluates the similarity between two feature maps with spike fashion.
- We propose a novel coding scheme to optimize the temporal distribution of output spike trains that improves the performance and shortens the latency.

## II. RELATED WORK

### A. Conversion methods of DNN-to-SNN

Many researches have been proposed for efficient SNNs training [12], [13] and achieve certain effects. However, they usually suffer accuracy degradation compared to DNNs. One major reason is that the training algorithms only fit shallow SNNs with two or three layers but DNNs are much deeper with great feature extraction and information processing capability. To construct deep SNNs, an alternative way is converting trained DNNs to SNNs with the same topology.

In the early stage work, Cao *et al.* [14] convert DNNs to SNNs and achieve excellent performance. They propose a comprehensive conversion scheme that can convert most modules in CNN-based networks except bias, batch normalization (BN), and max-pooling layers. Diehl *et al.* [15] suggest a data-based normalization method to enable a sufficient firing rate and achieve nearly lossless accuracy on MNIST [33] compared to DNNs.

In the subsequent work, Rueckauer *et al.* [16] demonstrate that merging the BN layer to the preceding layer is lossless and introduce spike max-pooling. Sengupta *et al.* [21] introduce a novel spike-normalization method for generating an SNN with deeper architecture and experiment on complex standard vision dataset ImageNet [34]. These methods have achieved comparable performance to DNNs in image classification.

As for other vision tasks, Kim *et al.* [18] propose channel-wise normalization (abbreviated to channel-norm) to upgrade

the firing rate and signed neuron with imbalanced threshold to express leaky-ReLU in the SNN domain. They first apply deep SNN to object detection successfully. Luo *et al.* [35] show the possibility to construct a deep SNN for object tracking on some simple videos. But they lack effective methods and convincing performance on the benchmark. PySpike [36] can measure the distance between two single spike trains, however, it brings complex computational consumption in large feature maps of deep SNNs, which makes it hard to run in real-time.

### B. Spike coding

Spike coding is the method of representing information with spike trains. Rate and temporal coding are the most frequently used coding schemes in SNNs.

Rate coding is based on the spike firing rate, which is used as the signal intensity, counted by the number of spikes occurred during a period. Thus, it has been widely used in converted SNNs [14], [16], [37] for classification by comparing the firing rates of each category. However, rate coding requires a higher latency for more accurate information [38]. For example, 512 time steps are needed to represent the positive integer 512. To represent 0.006, 6 spikes and 1000 time steps are required. As a result, rate coding is inefficient in terms of information transmission because of its redundancy, which leads to a long latency and energy consumption in deep SNNs.

Temporal coding uses timing information to mitigate long latency. Time-to-first-spike [39] only utilizes the arrival time of the first spike during a certain time. And many other coding schemes exploiting temporal information, such as rank-order coding [40] and phase coding [41]. Based on these, Kim *et al.* [42] propose weighted spikes by the phase function to make the most of the temporal information. Park *et al.* [17] introduce a burst coding scheme inspired by neuroscience research and investigates a hybrid coding scheme to exploit different features of different layers in SNNs.

### C. Object tracking

Object tracking aims to estimate the position of an arbitrary target in a video sequence while its location only initializes in the first frame by a bounding box. Trackers usually learn a model of the object's appearance and match with the candidate image in the current frame to determine the location by maximum response point. Tracking scenarios often appear occlusions, out-of-view, deformation, background cluttering, and other variations, which makes object tracking more challenging [43].

Two main branches of recent trackers are based on correlation filter (CF) [44], [45] and DNNs [46], [47]. CF trackers train regressors in the Fourier domain and update the weights of filters to do online tracking. Trackers based on DNNs are trained end-to-end and off-line, which enhance the richness of the model by big data sets. Motivated by CF, trackers based on Siamese networks with similarity comparison strategy have drawn great attention due to their high performance. SiamFC [3] introduces the correlation layer rather than fully

connected layers to evaluate the regional feature similarity between two frames, which highly improves the accuracy.

Many researches focus on improving the precision of the Siamese network and get state-of-the-art results. SiamRPN [48] adopts a region proposal network (RPN [49]) after a Siamese network and enhance tracking performance, the object tracking task is decomposed into classification and regression problem with correlation operation. SiamRPN++ [26] proposes a new model architecture to perform layer-wise and depth-wise aggregations and successfully train a Siamese tracker with deeper CNNs. Li *et al.* [27] investigate a method to enhance tracking robustness and accuracy by learning target-aware features.

For the aspect of energy and memory consumption, Liu *et al.* [50] construct small, fast yet accurate trackers by a teacher-students knowledge distillation model. Przewlocka *et al.* [51] aim to optimize SiamFC for memory and computational complexity through quantization, which shall directly translate into meeting real-time requirements via an FPGA implementation. To exploit the low-powered nature of SNNs, Yang *et al.* [52] propose a hybrid paradigm of ANN and SNN for efficient high-speed object tracking. And Cao *et al.* [53] design a three-layer SNN to perform simple tracking on a mobile robot.

### III. BACKGROUND

SiamFC [3] first introduces the correlation layer to calculate the response map with a representative Siamese architecture. Many state-of-the-art Siamese trackers are based on it for subsequent optimization. The concise but efficient network of SiamFC facilitates analyzing the proper SNN form of the similarity estimation in the correlation layer. Therefore, We select it as our base model.

SiamFC learns a function  $f(z, x)$  to compare an exemplar image  $z$  to candidate images  $x$  and computes the similarity at all sub-windows on a dense grid in a single evaluation. It obtains a response map and estimates the target position through the largest response value.

$$f(z, x) = \varphi(z) * \varphi(x) + b \cdot \mathbb{1}, \quad (1)$$

In Eq. 1, function  $\varphi$  performs feature representation and discriminator learning and  $b \cdot \mathbb{1}$  denotes a bias equated in every location.

Different from DNNs, SNNs use event-driven binary spike trains in a certain period rather than a single continuous value between neurons. The widely used integrate-and-fire (IF) neuron model integrates post-synaptic potential (PSP) into the membrane potential  $V_{\text{mem}}$ . In other words, the spiking neuron  $i$  accumulates the input  $z$  into the membrane potential  $V_{\text{mem},i}^l$  in the  $l$ th layer at each time step, which is described as

$$V_{\text{mem},i}^l(t) = V_{\text{mem},i}^l(t-1) + z_i^l(t) - V_{\text{th}}(t)\Theta_i^l(t), \quad (2)$$

where  $\Theta_i^l(t)$  is a spike in the  $i$ th neuron in the  $l$ th layer,  $V_{\text{th}}(t)$  is a certain threshold, and  $z_i^l(t)$  is the input of the  $i$ th neuron in the  $l$ th layer, which is described as

$$z_i^l(t) = \sum_j w_{ji}^l V_{\text{th}}(t)\Theta_j^{l-1}(t) + b_i^l, \quad (3)$$

where  $w^l$  is the weight and  $b^l$  is the bias in the  $l$ th layer. Each neuron will generate a spike only if its membrane potential exceeds a certain threshold  $V_{\text{th}}(t)$ . The process of spike generation can be generalized as

$$\Theta_i^l(t) = U(V_{\text{mem},i}^l(t-1) + z_i^l(t) - V_{\text{th}}(t)), \quad (4)$$

where  $U(\cdot)$  is a unit step function. Once the spike is generated, the membrane potential is reset to the resting potential. As shown in Eq. 2, we adopt the method of resetting by subtraction rather than resetting to zero, which increases firing rate and reduces the loss of information. The firing rate is defined as

$$\text{firing rate} = \frac{N}{T}, \quad (5)$$

where  $N$  is the total number of spikes during a given period  $T$ . The maximum firing rate will be 100% since the neuron generates a spike at each time step. Spike coding is the method of representing information with spike trains and different coding schemes cause various firing rates. A typical coding scheme is that input layer with real coding (real value) and hidden layers with rate coding [17].

In the early stage, converting deep ANNs into SNNs with less performance loss requires elaborate choices of parameters for spiking neurons such as firing rates and thresholds. Thus, We adopt layer-wise normalization (abbreviated to layer-norm) [16], a weight and threshold balancing method to prevent the neuron from over- or under-activation, the normalized weights and biases are calculated by

$$\tilde{w}^l = w^l \frac{\lambda^{l-1}}{\lambda^l} \quad \text{and} \quad \tilde{b}^l = \frac{b^l}{\lambda^l}, \quad (6)$$

where  $w$  are the weights of the original DNN,  $b$  are the biases, and  $\lambda$  is the 99.9th percentile of the maximum activation in the layer  $l$ . By these methods, function  $\varphi$  in Eq. 1 can be converted to a spiking convolutional neural network.

## IV. PROPOSED METHODS

### A. Model overview

We detail the SiamSNN, the converted SiamFC in Fig. 1. SiamSNN consists of a converted Siamese spiking convolutional neural network, two-status coding scheme, and an optimized hybrid similarity estimation method (potential and temporal correlation). The principles of spiking convolutional neural networks can be referred to Eq. 2,3,4,6. The hybrid similarity estimation method calculates the response map with the potential and temporal correlation of spike features. The two-status coding scheme optimizes the temporal distribution of output spike trains to improve the performance.

### B. Analysis of firing rates

Similar to the softmax layer, we can simply infer the response map output from the correlation computed on the membrane potentials of the last layer over the entire time. Hence, Eq. 1 can be changed into a spiking form:

$$M_P(z, x) = \left( \sum_{t=1}^T \varphi(z(t)) \right) * \left( \sum_{t=1}^T \varphi(x(t)) \right), \quad (7)$$

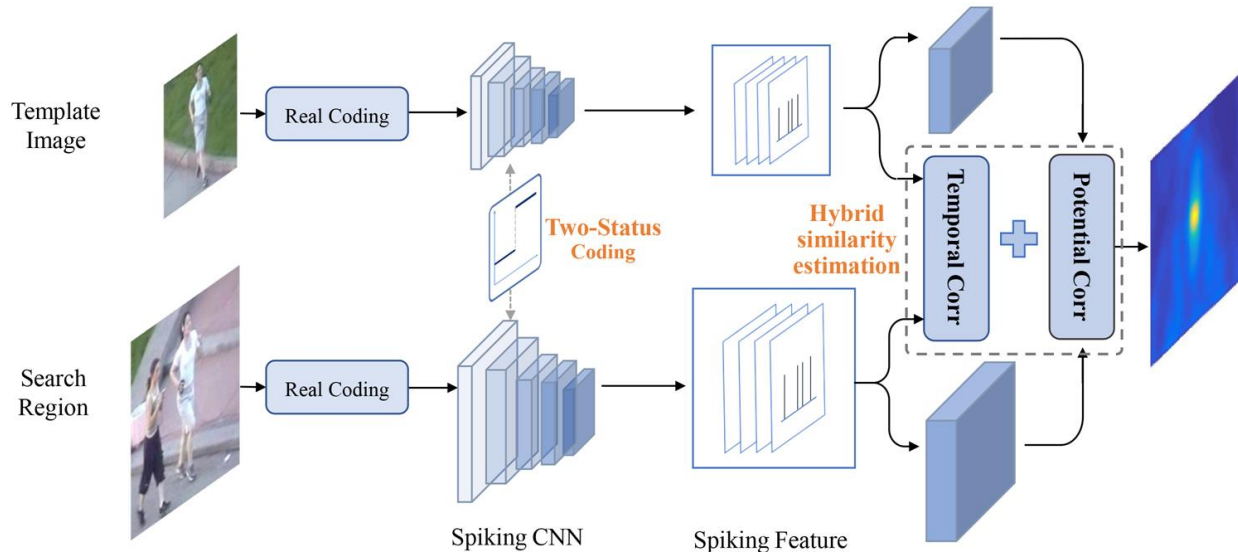


Fig. 1: **Framework of SiamSNN.** This framework consists of a converted Siamese spiking convolutional neural network, two-status coding scheme, and an optimized hybrid similarity estimation method (potential and temporal correlation). The hybrid similarity estimation method calculates the response map which denotes the similarity score between the template and the search region and the maximum of the response value indicates the target position. The two-status coding scheme optimizes the temporal distribution of output spike trains.

where  $M_P$  is the potential response map,  $z(t)$  and  $x(t)$  are the input encoded spike trains of exemplar image and candidate image,  $\varphi$  is the spiking convolutional embedding function,  $T$  is the latency. In the rest of the paper, we will refer to this simple method as potential similarity estimation (PSE).

We preliminary test PSE with layer-norm and rate coding on OTB-2013, unfortunately, it suffers from severe performance degradation. One of the main reasons for dropping performance is a reduction in firing rates on higher layers [37]. To enhance the efficiency of the information transmission, many researches aim at increasing the firing rate to an appropriate extent, due to a larger number of spikes incurs more dynamic energy consumption and significantly diminishes the merit of low energy consumption in deep SNNs [42]. Channel-norm [18] ensure the information transmission of small activations, which is beneficial in the deep layers for the regression problem.

Therefore, we analyze the impact of firing rates with different methods on tracking accuracy. Firstly we reference channel-norm to improve the information transmission for preventing under-activation and deploy it with rate coding. Then we implement phase coding [42] in the hidden layers to upgrade firing rates by generating a group of periodic spike trains. Additionally, we also compare to burst coding [17], the method makes neurons generating a group of short-ISI spikes for transmitting information efficiently. These methods show remarkable performance in image classification or object detection. We illustrate the comparative results in Table I and the firing rates in Fig. 2.

Although these advanced methods result in relatively high firing rates and efficient information transmission, they don't significantly improve accuracy degradation. Even channel-norm causes more loss of accuracy. It is indicated that only a few convolutional filters are active in describing the target in tracking and others contain irrelevant and redundancy informa-

TABLE I: The area under the curve (AUC) of success plots on OTB-2013 dataset with SiamFC and different configurations of SiamSNN+PSE

SiamFC	layer-norm + rate coding	channel-norm + rate coding	layer-norm + burst coding	layer-norm + phase coding
59.19	47.35	45.12	48.23	48.03

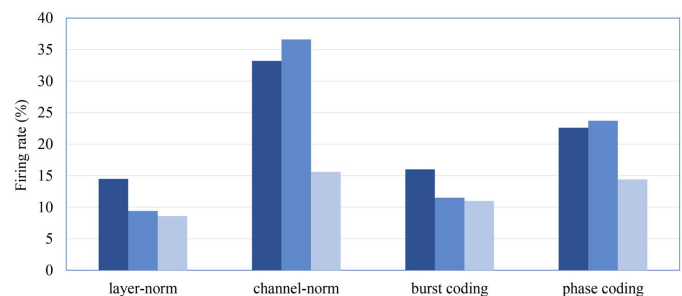


Fig. 2: Average firing rates of the four methods in conv1-3 on a test sequence of OTB-2013.

tion because inter-class differences are mainly related to a few feature channels [27]. In the process of similarity estimation, trackers determine the target position at the relatively largest response value, while small value at the background. For this reason, channel-norm enhances the activations of all channels that change the similarity gap between foreground and background, which brings more irrelevant information to obstruct tracking. Meanwhile, phase coding and burst coding have not discriminatively enhanced the spiking representation of the foreground target that improves little performance.

Our in-depth analysis demonstrates the potential impacts of firing rate on object tracking. Despite the efficient information transmission in spiking convolutional embedding function  $\varphi$  with these advanced methods, there is still a big accuracy

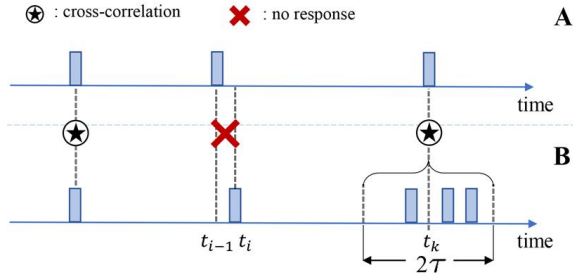


Fig. 3: Illustration of temporal correlation between spike train A and B.

gap between SiamSNN and SiamFC. In this case, we expect to optimize the process of correlation on the SNN domain. Moreover, temporal information of spike trains is the main difference between DNNs and SNNs, which makes an important impact on information transmission in SNNs [42], [20]. Motivated by this, we attempt to exploit temporal information in the similarity estimation method and coding scheme for further improvement.

### C. Hybrid spiking similarity estimation

Besides potential similarity, we can also match the temporal similarity between spiking features of exemplar and candidate images as

$$M_T(z, x) = \sum_{t=1}^T (\varphi(z(t)) * \varphi(x(t))), \quad (8)$$

which is similar to Eq. 7,  $M_T$  is the temporal response map. It calculates the correlation at each time step. In the rest of the paper, we will refer to this simple method as temporal similarity estimation (TSE).

Intuitively, rely on the alignment of spikes at each time step, TSE causes strict temporal consistency of correlation, which can also lead to a large drop of accuracy in actual measurement. For instance in Fig. 3, if spike train A of a pixel has spikes at  $t_{i-1}$ , and spike train B has spikes at  $t_i$ , their temporal correlation is 0 during  $(t_{i-2}, t_{i+1})$ , but intuitively they are highly similar. The measures of spike train synchrony in [36] also show a high similarity of the above two spike trains. Therefore, we optimize TSE and introduce a response period with time weights to solve this issue. It is defined as:

$$M_{\Delta\tau}(z, x) = \sum_{t=1}^T \sum_{m=t-\tau}^{t+\tau} \left( \frac{\varphi(z(m)) * \varphi(x(t))}{2|t-m|+1} \right), \quad (9)$$

where  $\tau$  is the response period threshold. We set  $\tau = 1$  by experiments, and the impacts of  $\tau$  are analyzed in Fig. 6 of Section V-B. As shown in Fig. 3, Eq. 9 makes spike trains A response with B during  $[t_k - \tau, t_k + \tau]$ . The response value will attenuate gradually when the time steps far from  $t_k$ . There is a trade-off between computation consumption and period threshold, and a longer period has few contributions to the response value. Thus,  $\tau$  is usually set to a small number.

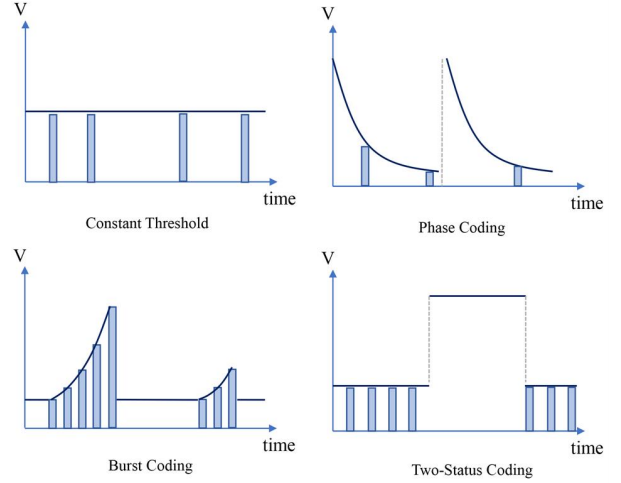


Fig. 4: Example of several coding methods with constant threshold, phase coding, burst coding and two-status coding. The solid lines express the effect of spiking on voltage threshold.

Considering PSE performs lossless on portions of sequences in OTB-2013, we calculate the final response map as follows:

$$f_{spike}(z, x) = \frac{1}{T^2} M_P(z, x) + \frac{1}{2T \cdot 2\tau} M_{\Delta\tau}(z, x) + b \cdot \mathbb{1}, \quad (10)$$

where the weights of  $M_P$  and  $M_{\Delta\tau}$  aim to normalize them to the same magnitude,  $b \cdot \mathbb{1}$  denotes the same bias in SiamFC. Noted that in SiamFC,  $f(z, x)$  compares an exemplar image  $z$  to a candidate image  $x$  in the current frame of the same size. It generates a high value if the two images describe the same object and low otherwise. And  $f_{spike}(z, x)$  is to simulate this function, not strictly calculates the similarity between two spike trains (e.g., the similarity equals 1 between two zero spike trains). It is the reason for choosing  $T$  instead of spike numbers as the normalization parameter to get response value.

It is worth noting that almost all tracking models based on Siamese networks have the correlation layer, and many of them obtain state-of-the-art results [26], [27]. The proposed method makes it possible to convert these remarkable trackers into deep SNNs. Our approaches provide a reference for similarity estimation of spike trains in deep SNNs. In the rest of the paper, we will refer to hybrid spiking similarity estimation as HSE.

### D. Two-status coding scheme

Although Eq. 10 enhances the temporal correlation between two spike trains, the temporal distributions of spikes are random and disorganized, which makes a large portion of spike values underutilized. We expect that the output spike of each time step will contribute to the final response value, which shortens latency for reducing energy consumption.

Phase coding [42] makes full use of the temporal information of spike trains, implemented by changing voltage threshold  $V_{th}(t)$  depending on the phase of the global reference clock, which cyclically produces spikes with a phase value. The function of it is given by

$$V_{th}(t) = 2^{-(1 + \text{mod}(t-1, K))} \quad (11)$$

where  $K$  is the period of the phase. Phase coding needs only  $K$  time steps to represent  $K$ -bit data (8-bit images usually) whereas rate coding would require  $2^K$  time steps to represent the same data.

Burst coding [17] is another advanced coding scheme, which generates a group of short-ISI spikes by increasing voltage thresholds exponentially if neurons spike continuously. Although these two methods gain little effect in object tracking as mentioned before, it follows that assigning periodicity to spike trains promotes their ability of information transmission, which brings efficient performance in image classification. To this end, we expect for periodic spiking feature when estimating the similarity.

Motivated by the neural phenomenon that repetitive electrical activity can induce a persistent potentiation or depression of synaptic efficacy in various parts of the nervous system (LTP and LTD) [29], we propose two-status coding scheme (hereinafter abbreviated as two-status coding), which represents the voltage threshold of potentiation status and depression status. We define the function as follows:

$$V_{th}(t) = \begin{cases} \alpha & \text{if } \text{mod}(t/p, 2) = 1 \\ \beta & \text{otherwise,} \end{cases} \quad (12)$$

where  $\alpha \rightarrow +\infty$  to prevent neurons from generating spikes during depression status and  $\beta$  is often smaller than the normalized voltage threshold 1 to excite neurons spiking during potentiation status,  $p$  is a constant that controls the period of neuron state change,  $t$  is the current time step. We set  $p = 5$  by observation of experiments and  $\beta = 0.5$  by experiences in Section V-B.

We illustrate the mentioned coding methods in Fig. 4. Constant threshold generates spikes disorderly with stable values; phase coding changes the threshold weight periodically; burst coding fires a group of short-ISI spike with exponentially increasing values. Our approach makes neurons fire with the same value in potentiation status and accumulates membrane potential in depression status. Two-status coding constrains equivalent spikes in a fixed periodic distribution, increase the density of spikes in potentiation status to enhance response value. Fig. 5 shows the distribution of spikes after two-status coding from the original rate coding. The proposed method can also save energy by avoiding neurons generating spikes which are useless for HSE. Moreover, spiking neurons in the next layer are not consuming energy during depression status due to zero input.

Park *et al.* [17] propose a hybrid coding scheme on input and hidden layers by the motivation that neurons occasionally use different neural coding schemes depending on their roles and locations in the brain. Inspired by this idea, we use two-status coding scheme for the output layer to optimize the temporal distribution of output spike trains, rate coding in hidden layers. And real coding for the input layer due to its fast and accurate features.

## V. EXPERIMENTS

### A. Datasets

We evaluate our methods on OTB-2013 [30], OTB-2015 [31], and VOT2016 [32]. The simulation and implemen-

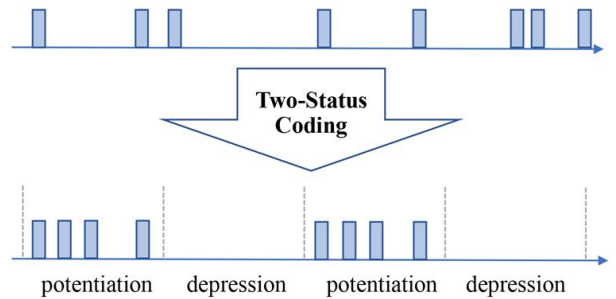


Fig. 5: The distribution of spikes after two-status coding from the original rate coding.

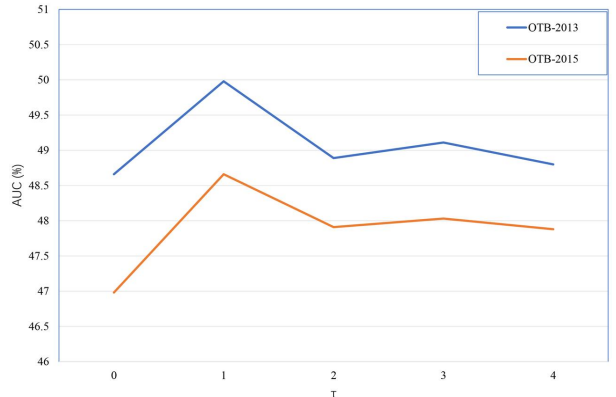


Fig. 6: Experimental results for different values of response period threshold on OTB-2013 and OTB-2015.

tations are based on TensorFlow.

To assess and verify the proposed methods, we use the overlap ratio (OR) as the basic metric firstly. OR is the Intersection over Union (IoU) between the tracked bounding box and ground truth bounding box, which is calculated based on object detection challenge VOC [54]:

$$OR = \frac{\text{area}(O_t \cap O_{gt})}{\text{area}(O_t \cup O_{gt})} \quad (13)$$

OTB and VOT are the widely used tracking benchmarks, which contain varieties of tracking challenging about out-of-view, variation, occlusions, deformation, fast motion, rotation, and background cluttering. OTB datasets adopt overlap score and center location error as their base metrics. The success plot shows the ratios of successful frames whose overlap ratio is larger than a given threshold. The precision plot measures the percentage of frames whose center location error in the range of a certain threshold. The area under the curve (AUC) of the success plot is usually used to rank tracking algorithms. As for VOT, the performance is evaluated in terms of accuracy (average overlap) and robustness (failure times). The overall performance is evaluated through Expected Average Overlap (EAO) which takes account of both accuracy and robustness.

### B. Experimental settings

In the evaluations, we firstly determine the hyperparameters of the proposed methods. Since the far-distance spikes have poor correlation, Fig. 6 compares the results for several small

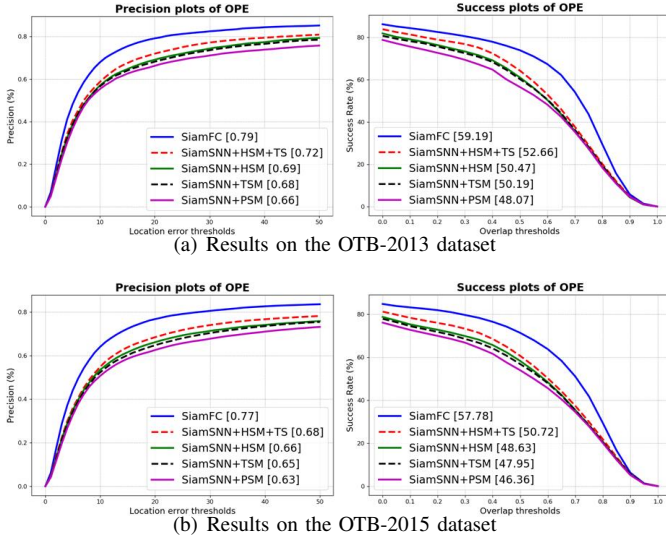


Fig. 7: Success and precision plots on the OTB-2013 and OTB-2015 datasets.

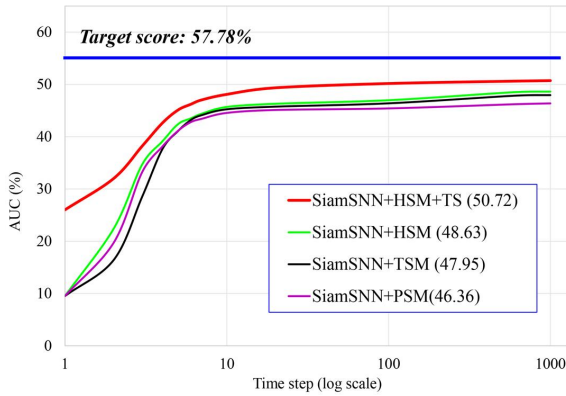


Fig. 8: Results of SiamSNN on different configurations evaluated by latency and the AUC of success plots on OTB-2015.

values of response period threshold  $\tau$  on OTB-2013 and OTB-2015. Thus,  $\tau$  is set to 1. As mentioned before in the two-status coding scheme, we set  $\alpha \rightarrow +\infty$  ( $\alpha = \text{float}('Inf')$  in python code) to prevent neurons from generating spikes during depression status. Refer to the exponential change of voltage threshold in burst coding [17], we set  $\beta$  to 0.5 to excite neurons spiking during potentiation status. It is inappropriate to set  $\beta$  to smaller values (e.g., 0.25 and 0.125), which will alter the balanced normalization in Eq. 3.6 and cause worse results.

The latency requirements are presented in Fig. 8, we can see that SiamSNN converges rapidly in 10 time steps and then rises slowly. So in the two-status coding (abbreviated to TS), we choose the state period  $p$  as 5 to improve the performance in shorter latency. To reach the maximum AUC, SiamSNN+HSE+TS requires approximately 20 time steps.

### C. Tracking results

**OTB-2015 Dataset.** We compare different configurations of SiamSNN with SiamFC and compute the average OR across all the videos of various the challenges on OTB100 for further analysis as shown in Table II. The challenges are

abbreviated as follows: background clutters (BC), deformation (DEF), fast motion (FM), in-plane rotation (IPR), illumination variation (IV), low resolution (LR), motion blur (MB), occlusion (OCC), out-of-plane rotation (OPR), out-of-view (OV), scale variation (SV). SiamSNN+HSE+TS achieves the least accuracy degradation (5.5%) compared to SiamFC (61.7% vs. 67.2%).

We find that SiamSNN will reduce accuracy more or less in each type of tracking challenge attributes, especially in low resolution (LR) and out-of-view (OV). We choose some videos for in-depth analysis. Fig. 9 depicts the tracking results of three trackers (SiamFC, SiamSNN+PSE, and SiamSNN+HSE+TS) in several challenging sequences. Si-amSNN has almost the same performance as SiamFC in most simple tracking scenarios. However the converted spike-based model will have weaker discrimination abilities, it is likely to make wrong precisions in case of challenging scenarios.

In occlusion, motion blur, and scale variation, the performance of SiamSNN+HSE+TS is closer to SiamFC than SiamSNN+PSE. PSE often drifts the target when heavy occlusions and scale variations occur in car1, david3, human7, jogging1.

In background clutters, plane rotation, fast motion, both SiamSNN and SiamFC will drift off the target when encountering challenging circumstances. So that SiamSNN unexpectedly performs well than SiamFC in the basketball sequence, and they all drift away in the bolt2 and skating2-1 sequence.

In low resolution, out-of-view, although SiamSNN can scarcely track the target in the sequences of lemming, surfer, and tiger1, the bounding boxes always deviate from ground truths.

For further evaluation, we measure the precision and success plots of OPE on OTB-2013 and OTB-2015. As depicted in Fig. 7, the target AUC of precision and success plots in SiamFC are 79%, 59.19% (OTB-2013) and 77%, 57.78% (OTB-2015). And our SiamSNN achieves 72%, 52.66% (OTB-2013) and 68%, 50.72% (OTB-2015). SiamSNN+HSM+TS achieves outstanding performance improvement than other configurations. We choose this optimal configuration for the rest of our experiments. However, SiamSNN often drifts off the target when encountering complex circumstances due to the loss of discriminative features in the conversion of DNN-to-SNN.

**VOT2016 Dataset.** On the OTB benchmark, the overlap ratio will drop sharply once SiamSNN drifts off the target since the tracker will not be reset. This is the main reason for SiamSNN suffering a relatively large gap with SiamFC. Thus, we compare SiamSNN with other algorithms on VOT2016. In this experiment, the proposed method is compared to the works in the same period of SiamFC: SRBT [55], DPT [56], KCF [57], EBT [58]. Besides, SiamRPN [48] is added for comparison, which is a more advanced Siamese tracker than SiamFC.

As shown in Table III, compared to SiamFC, the accuracy of SiamSNN only drops 3.2% but the robustness becomes poor, and the degradation of EAO is 2.3%. Our method achieves comparable performance to other trackers. We aim at studying the spiking representation of SiamRPN in the next step.

TABLE II: The average overlap ratio across all the videos of various the challenges on OTB100, about the four configuration of SiamSNN and SiamFC.

overlap(%)	ALL	BC	DEF	FM	IPR	IV	LR	MB	OCC	OPR	OV	SV
SiamFC	67.2	65.4	62.2	67.4	66.4	65.6	69.3	69	65.5	65.5	66.6	66.4
SiamSNN+PSE	59.6	56.3	54.9	59.2	60.2	56.1	62	63.4	58.7	57.1	56.2	57.3
SiamSNN+TSE	60.4	56.7	56.7	61.4	61.4	56.9	57.4	63.8	59.6	57.9	54.2	57.7
SiamSNN+HSE	60.5	56.8	57.6	60.8	60.7	56.5	57.3	63.6	60.4	57.8	53.9	58
SiamSNN+HSE+TS	<b>61.7</b>	59.9	58.4	61.3	61.6	59.8	59.5	64	61.1	59.8	54.8	59.1



Fig. 9: Tracking results on 10 sequences of OTB-2015 (from left to right and top to down are basketball, bolt2, car1, david3, human7, jogging1, lemming, skating2-1, surfer, tiger1). The indexes are shown in the top left of each frame.

TABLE III: Comparison results about SiamSNN with other trackers on VOT2016.

	A	R	EAO
SiamRPN	<b>0.560</b>	0.26	<b>0.344</b>
SiamFC (origin)	0.529	0.49	0.233
<b>SiamSNN (ours)</b>	0.497	0.63	0.210
SRBT	0.496	0.35	0.290
DPT	0.492	0.49	0.236
KCF	0.489	0.57	0.192
EBT	0.465	<b>0.25</b>	0.291

D. Energy consumption and latency evaluation

This is the first work that reports the competitive performance of SNNs for object tracking on OTB-2013, OTB-2015, and VOT2016 datasets. Therefore, we compare it with other state-of-the-art SNN methods on image classification and object detection in terms of accuracy decline and latency as shown in Table IV.

Recently the SNN achieves comparable accuracy with that of DNN for the MNIST dataset and only require short latency. In the case of the CIFAR-100 dataset, a larger dataset for classification, SNNs obtain the accuracy close to the DNN when applying phase coding or burst coding. But they demand

3000 time steps. Sengupta *et al.* [21] apply the SNN on the entire 50,000 ImageNet 2012 validation set. Although the accuracy degradation of the SNN to original DNN is 5.22% and with 2500 time steps, it is the first work to demonstrate the competitive performance of a conversion-based SNN on ImageNet data for deep neural architectures. It follows that the SNNs decline more accuracy when applied to large and complex datasets. As for object detection tasks, Spiking-YOLO [18] achieves remarkable results with 3500 time steps on non-trivial datasets, PASCAL VOC and MS COCO. It is worth noting that our SiamSNN reaches 20 time steps on object tracking, a relatively remarkable performance of latency, which provides great possibilities to achieve real-time on neuromorphic chips.

We estimate energy consumption and speed from neuromorphic chips (TrueNorth [6]) to investigate the effect of our methods and compare them to SiamFC, SiamRPN++, and DSTfc. Bertinetto *et al.* [3] run SiamFC(3s) on a single NVIDIA GeForce GTX Titan X (250 Watts) and reach 86 FPS (11.63ms per frame). SiamRPN++ [26] has a more network architecture and also state-of-the-art performance, which is able to run at 35 FPS (28.57ms per frame) on NVIDIA Titan Xp GPU (250 Watts). And DSTfc [50], a small, fast yet accurate tracker by teacher-students knowledge distillation, is running at 230 FPS (4.35ms per frame) on Nvidia GTX 1080ti

TABLE IV: Comparison of inference results with other state-of-the-art SNN methods on various vision tasks datasets.

Problems	Dataset	Methods	Network	Coding	DNN Acc.(%)	SNN Acc.(%)	Acc. Loss	Latency
Image Classification	MNIST	Diehl <i>et al.</i> 2015 [15]	CNN	rate	99.14	99.10	0.04	200
		Kim <i>et al.</i> 2018 [42]	CNN	phase	99.20	99.20	0	16
		Park <i>et al.</i> 2019 [17]	CNN	burst	99.25	99.25	0	87
	CIFAR-100	Kim <i>et al.</i> 2018 [42]	VGG-16	phase	68.77	68.37	0.4	3000
		Park <i>et al.</i> 2019 [17]	VGG-16	burst	68.77	68.69	0.08	3000
		Sengupta <i>et al.</i> 2019 [21]	ResNet-34	rate	70.69	65.47	5.22	2500
Object Detection	PASCAL VOC	Kim <i>et al.</i> 2019 [18]	YOLO	rate	53.01	51.83	1.18	3500
	MS COCO	Kim <i>et al.</i> 2019 [18]	YOLO	rate	26.24	25.66	0.58	3500
Object Tracking	OTB-2015	<b>SiamSNN+HSE+TS</b>	CNN	<b>two-status</b>	67.2	61.7	5.5	<b>20</b>
	VOT-2016	<b>SiamSNN+HSE+TS</b>	CNN	<b>two-status</b>	52.94	49.67	3.27	<b>20</b>

TABLE V: Comparison of speed and energy consumption of SiamFC and SiamSNN

Methods	FLOPs /SOPS	Power (W)	Time (ms)	Energy (J)
SiamRPN++	1.42E+10	250	28.57	7.14
SiamFC	5.44E+09	250	11.63	2.91
DSTfc	–	250	4.35	1.10
SiamSNN	<b>3.94E+08</b>	9.85E-04	20	<b>1.97E-05</b>

GPU (250 Watts).

TrueNorth measures computation by synaptic operations per second (SOPS) and can deliver 400 billion SOPS per Watt, while floating-point operations per second (FLOPS) in modern supercomputers. And the time step is nominally 1ms, set by a global 1kHz clock [6]. We count the operations with the formula in [16].

The calculation results of processing one frame are presented in Table V. The energy consumption of SiamSNN on TrueNorth is extremely lower than SiamFC on GPU. Although GPUs are far more advanced computing technology, it is hard to employ DNNs on embedded systems through them. Neuromorphic chips with higher energy and computational efficiency have a promising development and application. We expect that our SiamSNN can be implemented on embedded systems and applied widely in CV scenarios.

## VI. CONCLUSION

In this paper, we propose SiamSNN, the first deep SNN model for object tracking that reaches competitive performance to DNNs with short latency and low precision loss on OTB-2013, OTB-2015, and VOT2016 datasets. Our analysis indicates that enhancing the firing rates of all neurons has no significant contribution to object tracking. Consequently, we propose an optimized hybrid spiking similarity estimation method and a two-status coding scheme for taking full advantage of temporal information in spike trains, which achieves real-time on TrueNorth. We believe that our methods can be applied in more spiking Siamese networks for tracking and other similarity estimation problems.

## REFERENCES

[1] A. Krizhevsky, I. Sutskever, and G. E. Hinton, “Imagenet classification with deep convolutional neural networks,” in *Advances in neural information processing systems*, 2012, pp. 1097–1105.

[2] J. Redmon, S. Divvala, R. Girshick, and A. Farhadi, “You only look once: Unified, real-time object detection,” in *Proceedings of the IEEE conference on computer vision and pattern recognition*, 2016, pp. 779–788.

[3] L. Bertinetto, J. Valmadre, J. F. Henriques, A. Vedaldi, and P. H. Torr, “Fully-convolutional siamese networks for object tracking,” in *ECCV*. Springer, 2016, pp. 850–865.

[4] X. Yu, T. Liu, X. Wang, and D. Tao, “On compressing deep models by low rank and sparse decomposition,” in *CVPR*, 2017, pp. 7370–7379.

[5] Y. Wei, X. Pan, H. Qin, W. Ouyang, and J. Yan, “Quantization mimic: Towards very tiny cnn for object detection,” in *ECCV*, 2018, pp. 267–283.

[6] P. A. Merolla, J. V. Arthur, R. Alvarez-Icaza, A. S. Cassidy, J. Sawada, F. Akopyan, B. L. Jackson, N. Imam, C. Guo, Y. Nakamura *et al.*, “A million spiking-neuron integrated circuit with a scalable communication network and interface,” *Science*, vol. 345, no. 6197, pp. 668–673, 2014.

[7] M. Davies, N. Srinivasa, T.-H. Lin, G. Chinya, Y. Cao, S. H. Choday, G. Dimou, P. Joshi, N. Imam, S. Jain *et al.*, “Loihi: A neuromorphic manycore processor with on-chip learning,” *IEEE Micro*, vol. 38, no. 1, pp. 82–99, 2018.

[8] N. K. Kasabov, “Neucube: A spiking neural network architecture for mapping, learning and understanding of spatio-temporal brain data,” *Neural Networks*, vol. 52, pp. 62–76, 2014.

[9] S. Ghosh-Dastidar and H. Adeli, “Spiking neural networks,” *International journal of neural systems*, vol. 19, no. 04, pp. 295–308, 2009.

[10] W. Maass, “Networks of spiking neurons: the third generation of neural network models,” *Neural networks*, vol. 10, no. 9, pp. 1659–1671, 1997.

[11] A. Tavanaei, M. Ghodrati, S. R. Kheradpisheh, T. Masquelier, and A. Maida, “Deep learning in spiking neural networks,” *Neural Networks*, 2018.

[12] N. Caporale and Y. Dan, “Spike timing-dependent plasticity: a hebbian learning rule,” *Annu. Rev. Neurosci.*, vol. 31, pp. 25–46, 2008.

[13] Y. Jin, W. Zhang, and P. Li, “Hybrid macro/micro level backpropagation for training deep spiking neural networks,” in *Advances in Neural Information Processing Systems*, 2018, pp. 7005–7015.

[14] Y. Cao, Y. Chen, and D. Khosla, “Spiking deep convolutional neural networks for energy-efficient object recognition,” *International Journal of Computer Vision*, vol. 113, no. 1, pp. 54–66, 2015.

[15] P. U. Diehl, D. Neil, J. Binas, M. Cook, S.-C. Liu, and M. Pfeiffer, “Fast-classifying, high-accuracy spiking deep networks through weight and threshold balancing,” in *IJCNN*. IEEE, 2015, pp. 1–8.

[16] B. Rueckauer, I.-A. Lungu, Y. Hu, M. Pfeiffer, and S.-C. Liu, “Conversion of continuous-valued deep networks to efficient event-driven networks for image classification,” *Frontiers in neuroscience*, vol. 11, p. 682, 2017.

[17] S. Park, S. Kim, H. Choe, and S. Yoon, “Fast and efficient information transmission with burst spikes in deep spiking neural networks,” in *Design Automation Conference*. ACM, 2019, p. 53.

[18] S. Kim, S. Park, B. Na, and S. Yoon, “Spiking-yolo: Spiking neural network for real-time object detection,” *arXiv preprint arXiv:1903.06530*, 2019.

[19] Y. Wu, L. Deng, G. Li, J. Zhu, Y. Xie, and L. Shi, “Direct training for spiking neural networks: Faster, larger, better,” in *Proceedings of the AAAI Conference on Artificial Intelligence*, vol. 33, 2019, pp. 1311–1318.

[20] K. Roy, A. Jaiswal, and P. Panda, “Towards spike-based machine intelligence with neuromorphic computing,” *Nature*, vol. 575, no. 7784, pp. 607–617, 2019.

[21] A. Sengupta, Y. Ye, R. Wang, C. Liu, and K. Roy, “Going deeper in spiking neural networks: Vgg and residual architectures,” *Frontiers in neuroscience*, vol. 13, 2019.

- [22] J.-W. Hsieh, S.-H. Yu, Y.-S. Chen, and W.-F. Hu, "Automatic traffic surveillance system for vehicle tracking and classification," *IEEE Transactions on Intelligent Transportation Systems*, vol. 7, no. 2, pp. 175–187, 2006.
- [23] K.-H. Lee and J.-N. Hwang, "On-road pedestrian tracking across multiple driving recorders," *IEEE Transactions on Multimedia*, vol. 17, no. 9, pp. 1429–1438, 2015.
- [24] S. Tang, M. Andriluka, B. Andres, and B. Schiele, "Multiple people tracking by lifted multicut and person re-identification," in *Proceedings of the IEEE Conference on Computer Vision and Pattern Recognition*, 2017, pp. 3539–3548.
- [25] Z. Zhu, Q. Wang, B. Li, W. Wu, J. Yan, and W. Hu, "Distractor-aware siamese networks for visual object tracking," in *Proceedings of the European Conference on Computer Vision (ECCV)*, 2018, pp. 101–117.
- [26] B. Li, W. Wu, Q. Wang, F. Zhang, J. Xing, and J. Yan, "Siamrpn++: Evolution of siamese visual tracking with very deep networks," in *CVPR*, 2019, pp. 4282–4291.
- [27] X. Li, C. Ma, B. Wu, Z. He, and M.-H. Yang, "Target-aware deep tracking," in *CVPR*, 2019, pp. 1369–1378.
- [28] A. Basu, J. Acharya, T. Karnik, H. Liu, H. Li, J.-S. Seo, and C. Song, "Low-power, adaptive neuromorphic systems: Recent progress and future directions," *IEEE Journal on Emerging and Selected Topics in Circuits and Systems*, vol. 8, no. 1, pp. 6–27, 2018.
- [29] G.-q. Bi and M.-m. Poo, "Synaptic modifications in cultured hippocampal neurons: dependence on spike timing, synaptic strength, and postsynaptic cell type," *Journal of neuroscience*, vol. 18, no. 24, pp. 10464–10472, 1998.
- [30] Y. Wu, J. Lim, and M.-H. Yang, "Online object tracking: A benchmark," in *CVPR*, 2013, pp. 2411–2418.
- [31] Y. Wu, J. Lim, and M.-H. Yang, "Object tracking benchmark," *IEEE Transactions on Pattern Analysis and Machine Intelligence*, vol. 37, no. 9, pp. 1834–1848, 2015.
- [32] J. M. M. Kristan, A. Leonardis and et al, "The visual object tracking VOT2016 challenge results," in *ECCV 2016 Workshops*, 2016, pp. 777–823.
- [33] Y. LeCun, L. Bottou, Y. Bengio, and P. Haffner, "Gradient-based learning applied to document recognition," *Proceedings of the IEEE*, vol. 86, no. 11, pp. 2278–2324, 1998.
- [34] O. Russakovsky, J. Deng, H. Su, J. Krause, S. Satheesh, S. Ma, Z. Huang, A. Karpathy, A. Khosla, M. Bernstein *et al.*, "Imagenet large scale visual recognition challenge," *International journal of computer vision*, vol. 115, no. 3, pp. 211–252, 2015.
- [35] Y. Luo, Q. Yi, T. Wang, L. Lin, Y. Xu, J. Zhou, C. Yuan, J. Guo, P. Feng, and Q. Feng, "A spiking neural network architecture for object tracking," in *International Conference on Image and Graphics*. Springer, 2019, pp. 118–132.
- [36] M. Mulansky and T. Kreuz, "Pyspike-a python library for analyzing spike train synchrony," *SoftwareX*, vol. 5, pp. 183–189, 2016.
- [37] B. Rueckauer, I.-A. Lungu, Y. Hu, and M. Pfeiffer, "Theory and tools for the conversion of analog to spiking convolutional neural networks," *arXiv preprint arXiv:1612.04052*, 2016.
- [38] J. Gautrais and S. Thorpe, "Rate coding versus temporal order coding: a theoretical approach," *Biosystems*, vol. 48, no. 1-3, pp. 57–65, 1998.
- [39] S. Thorpe, A. Delorme, and R. Van Rullen, "Spike-based strategies for rapid processing," *Neural networks*, vol. 14, no. 6-7, pp. 715–725, 2001.
- [40] S. J. Thorpe, "Spike arrival times: A highly efficient coding scheme for neural networks," *Parallel processing in neural systems*, pp. 91–94, 1990.
- [41] C. Kayser, M. A. Montemurro, N. K. Logothetis, and S. Panzeri, "Spike-phase coding boosts and stabilizes information carried by spatial and temporal spike patterns," *Neuron*, vol. 61, no. 4, pp. 597–608, 2009.
- [42] J. Kim, H. Kim, S. Huh, J. Lee, and K. Choi, "Deep neural networks with weighted spikes," *Neurocomputing*, vol. 311, pp. 373–386, 2018.
- [43] M. Fiaz, A. Mahmood, S. Javed, and S. K. Jung, "Handcrafted and deep trackers: A review of recent object tracking approaches," *ACM Surveys*, 2018.
- [44] L. Bertinetto, J. Valmadre, S. Golodetz, O. Miksik, and P. H. Torr, "Staple: Complementary learners for real-time tracking," in *Proceedings of the IEEE conference on computer vision and pattern recognition*, 2016, pp. 1401–1409.
- [45] S. Moorthy, J. Y. Choi, and Y. H. Joo, "Gaussian-response correlation filter for robust visual object tracking," *Neurocomputing*, 2020.
- [46] D. Held, S. Thrun, and S. Savarese, "Learning to track at 100 fps with deep regression networks," in *ECCV*. Springer, 2016, pp. 749–765.
- [47] H. Hu, B. Ma, J. Shen, H. Sun, L. Shao, and F. Porikli, "Robust object tracking using manifold regularized convolutional neural networks," *IEEE Transactions on Multimedia*, vol. 21, no. 2, pp. 510–521, 2018.
- [48] B. Li, J. Yan, W. Wu, Z. Zhu, and X. Hu, "High performance visual tracking with siamese region proposal network," in *CVPR*, 2018, pp. 8971–8980.
- [49] S. Ren, K. He, R. Girshick, and J. Sun, "Faster r-cnn: Towards real-time object detection with region proposal networks," in *Advances in neural information processing systems*, 2015, pp. 91–99.
- [50] Y. Liu, X. Dong, W. Wang, and J. Shen, "Teacher-students knowledge distillation for siamese trackers," *arXiv preprint arXiv:1907.10586*, 2019.
- [51] D. Przewlocka, M. Wasala, H. Szolc, K. Blachut, and T. Kryjak, "Optimisation of a siamese neural network for real-time energy efficient object tracking," *arXiv preprint arXiv:2007.00491*, 2020.
- [52] Z. Yang, Y. Wu, G. Wang, Y. Yang, G. Li, L. Deng, J. Zhu, and L. Shi, "Dashnet: A hybrid artificial and spiking neural network for high-speed object tracking," *arXiv preprint arXiv:1909.12942*, 2019.
- [53] Z. Cao, L. Cheng, C. Zhou, N. Gu, X. Wang, and M. Tan, "Spiking neural network-based target tracking control for autonomous mobile robots," *Neural Computing and Applications*, vol. 26, no. 8, pp. 1839–1847, 2015.
- [54] M. Everingham, L. Van Gool, C. K. Williams, J. Winn, and A. Zisserman, "The pascal visual object classes (voc) challenge," *International journal of computer vision*, vol. 88, no. 2, pp. 303–338, 2010.
- [55] H. Lee and D. Kim, "Salient region-based online object tracking," in *2018 IEEE Winter Conference on Applications of Computer Vision (WACV)*. IEEE, 2018, pp. 1170–1177.
- [56] A. Lukežič, L. Č. Zajc, and M. Kristan, "Deformable parts correlation filters for robust visual tracking," *IEEE transactions on cybernetics*, vol. 48, no. 6, pp. 1849–1861, 2017.
- [57] J. F. Henriques, R. Caseiro, P. Martins, and J. Batista, "High-speed tracking with kernelized correlation filters," *IEEE transactions on pattern analysis and machine intelligence*, vol. 37, no. 3, pp. 583–596, 2014.
- [58] G. Zhu, F. Porikli, and H. Li, "Beyond local search: Tracking objects everywhere with instance-specific proposals," in *Proceedings of the IEEE conference on computer vision and pattern recognition*, 2016, pp. 943–951.